Reinvestigation of the Reactions of Camphorketene: Structural Evidence for Pseudopericyclic Pathways[1]

William W. Shumway,[†] N. Kent Dalley,*[,‡] and David M. Birney*[,†]

Department of Chemistry and Biochemistry, Texas Tech University, Lubbock, Texas 79409-1061 and Department of Chemistry and Biochemistry, C100 BNSN, Brigham Young University, Provo, Utah 84602

David.Birney@ttu.edu

Received April 19, 2001

The stereochemistry of the dimers (**3** and **4**) of camphorketene (**2**) have been determined. The crystal structures of **3**, **20** and of related compounds show ground-state distortions that are interpreted as prefiguring planar, pseudopericyclic transition states for retro-cycloadditions to form α-oxoketenes. The B3LYP/6-31G* optimized geometry for the transition structure (**10**) for the dimerization of *s-Z*-formylketene (**8**) is consistent with this mechanism. Trapping of **2** with alcohols shows selectivity comparable to other α-oxoketenes. The lack of reaction of **2** with benzaldehyde and the lack of enol tautomers in camphoric acid derivatives is attributed to angle strain in the bicyclic camphor moiety.

Introduction

As part of an ongoing study of reactions of α-oxoketenes in general and of their stereoselectivity in particular,[2] we became interested in the camphor-derived α-oxoketene **2**. Camphor is a readily available chiral compound and its derivatives often give excellent facial selectivity,[3] while α-oxoketenes exhibit unusual reactivity as compared to unsubstituted ketenes.[4] This work was undertaken to explore the interplay of the camphor and α-oxoketenes moieties in the reactivity of **2**. In determining the structure of **3** through X-ray crystallography, we also discovered structural evidence for the proposed planar, pseudopericyclic transition state for the dimerization of **2**. Examination of published X-ray structures of related adducts of α-oxoketenes also reveals that these compounds show similar distortions. These data are consistent with the geometries of the transition structures calculated at the B3LYP/6-31G* level.

Staudinger first generated camphorketene (**2**) by the treatment of the acid chloride **1** with triethylamine as in Scheme 1.[5] Two dimers were isolated in 45% and 21% yields. Later, Yates and Chandross deduced the general structures of dimers **3** and **4** but not their relative stereochemistry.[6]

Subsequently Wentrup et al. directly observed **2** by IR not only in argon matrices but also in solution at room temperature.[7] Methanol trapping of **2** yielded the esters

Scheme 1. Generation and Reactions of Camphorketene (2)

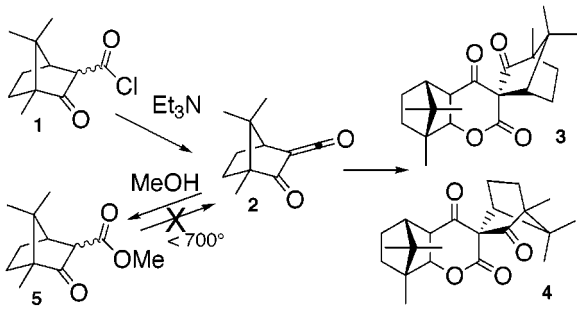

5. In contrast to other β-keto esters, the fragmentation of **5** to produce **2** was observed only at very high temperatures and in low yield.[7] This was attributed to the absence of the more reactive enol tautomer.[7]

Results and Discussion

In this work, we have verified the structure of dimer **3** by X-ray crystallography and have assigned the stereochemistry of **4** by NMR. We report chemoselective trapping of **2** by alcohols. However, **2** fails to undergo [4 + 2] cycloadditions with benzaldehyde and benzaldimine, a reaction that is characteristic of other α-oxoketenes. We attribute the observed lack of diastereoselectivity in the dimerization of **2** to the unhindered geometry of a planar, pseudopericyclic transition state as calculated at the B3LYP/6-31G* level of theory. The X-ray structures of **3** and of related compounds show ground-state distortions toward just such planar structures.

Using Staudinger's general procedure,[5] D-(+)-camphoric acid (**7**) was readily prepared by carboxylation of the lithium enolate of D-(+)-camphor. Subsequent treatment of **7** with $SOCl_2$ generated the acid chloride **1**. The camphorketene dimers **3** and **4** were then obtained upon treatment of the acid chloride **1** with triethylamine (Scheme 1). Successive recrystallization yielded pure **3** and **4**. The optical rotation of the minor dimer (α_D = +135°, $CHCl_3$) compares well with that originally re-

[†] Texas Tech University.
[‡] Brigham Young University.

(1) Taken in part from the Ph.D. dissertation of William W. Shumway, Texas Tech University, 2001.

(2) (a) Birney, D. M.; Xu, X.; Ham, S.; Huang, X. *J. Org. Chem.* **1997**, *62*, 7114−7120. (b) Shumway, W. W.; Ham, S.; Moer, J.; Wittlesey, B. R.; Birney, D. M. *J. Org. Chem.* **2000**, *65*, 7731−7739

(3) (a) Oppolzer, W. *Pure Appl. Chem* **1990**, *62*, 1241−1250. (b) Busacca, C. A.; Campbell, S.; Dong, Y.; Grossbach, D.; Ridges, M.; Smit, L.; Spinelli, E. *J. Org. Chem.* **2000**, *65*, 4753−4755.

(4) For reviews, see: (a) Wentrup, C.; Heilmayer, W.; Kollenz, G. *Synthesis* **1994**, 1219−1248. (b) Tidwell, T. T. *Ketenes*; John Wiley & Sons: New York, 1995.

(5) Staudinger, H.; Schotz, S. *Ber. Dtsch. Chem Ges.* **1920**, *53*, 1105−1124.

(6) Yates, P.; Chandross, E. A.; *Tetrahedron Lett.* **1959**, 1−6.

(7) Wentrup, C.; Freiermuth, B.; *J. Org. Chem.* **1991**, *56*, 2286−2289.

10.1021/jo015698t CCC: $20.00
Published on Web 07/25/2001

Scheme 2. Alcohol Trapping of Camphorketene 2

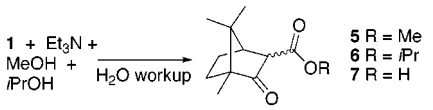

Table 1. Alcohol Trapping of Camphorketene 2[a]

	Et_3N:MeOH:*i*-PrOH	% **5**[b]	**5** endo:exo[b]	% **6**[b]	**6** endo:exo[b]	% **7**[b]
a	5:0:2	0		100	4.4:1	0
b	0:5:2	30	1.9:1	13	3.3:1	56
c	5:5:2	79	4:1	21	6:1	0

[a] Reaction conditions for reactions of **1** as in Scheme 2. All reactions were run under nitrogen atmospheres with freshly distilled diethyl ether as solvent. [b] Yield % and endo:exo ratios based on ^{1}H NMR integration of crude reactions.

ported by Staudinger ($\alpha_D = +126°$, EtOAc). X-ray analysis of this minor dimer confirmed the structure as **3**.[8] Although the major product decomposed readily,[6] its structure could be assigned as **4** by analogy to **3** and by comparison of the NMR spectra. Similar [4 + 2] dimerizations are observed for other α-oxoketenes.[4,9]

Conceivably, a [4 + 2] cycloaddition with a trap other than a ketene might lead to higher diastereoselectivity. Although benzaldehyde undergoes such cycloadditions with other α-oxoketenes,[2] its inclusion in the reaction sequence in Scheme 1 failed to produce any cycloadduct. The only products were those of camphor ketene dimerization. Imines are more reactive than aldehydes in trapping with other α-oxoketenes[10,11] so *N*-propylbenzaldimine was substituted for benzaldehyde in the previous reaction. This again gave dimers **3** and **4** but no evidence for reaction between **2** and the imine.

α-Oxoketenes are well-known to react rapidly with alcohols to produce *β*-keto esters.[4] When **2** is generated in the presence of 2-propanol, isopropyl 3-camphorcarboxylate (**6**) is formed (Scheme 2, Table 1). In 20 min this gave complete conversion to **6** (entry a, Table 1). However, in this reaction sequence the acid chloride precursor **1** can in principle be esterified directly to give the same product. To test the mechanism, a competition reaction was set up using 2-propanol and methanol as traps. A control reaction of **1** with an 2-propanol/methanol mixture (entry b) was run in parallel with a reaction of **1** with triethylamine and the same alcohol mixture (entry c). Both reactions were quenched with water after 20 min, at which time any unreacted **1** or **2** were converted to the acid **7**.

The control reaction (without Et_3N, entry b) produced **5**, **6**, and **7**, the latter indicating an incomplete reaction after 20 min. The absence of **7** in entries a and c indicates a faster reaction than entry b.[12] Furthermore the product ratio of esters **5** to **6** and the endo:exo ratio of products for entry b are different than for entry c. These results argue that the two reactions proceed by different mechanisms in the presence and absence of triethylamine, the former being much faster. Differing product and endo:exo ratios of **5** and **6** in entries b and c also indicate that the two reactions do not share a common reaction intermediate, consistent with ketene **2** as an intermediate for entries a and c and not direct esterification of the acid chloride **1**. Significantly, the more reactive α-oxoketene **2** (entry c) shows higher selectivity than does the acid chloride **1** (entry b), consistent with the selectivity observed in reactions of acetylketene.[2]

Scheme 3. Proposed [2 + 2] and [4 + 2] Pathways for the Formation of 5

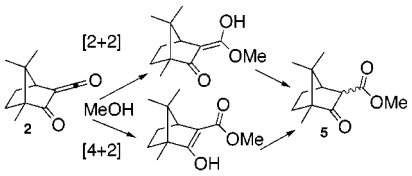

Hydration of ketene occurs via initial formation of the enol acid followed by subsequent tautomerization.[13] Hydration of α-oxoketenes normally occurs via a 6-centered transition state (calculated to be planar and pseudopericyclic[14]) to form the enol, followed by tautomerization to the *β*-ketoacid.[15] In the case of the reaction of camphorketene **2** with alcohols (Scheme 3), either the 4-centered or the 6-centered pathways are possible. Given that other [4 + 2] reactions of **2** are difficult, it may well be that the 4-centered pathway is followed. There is no evidence requiring the 6-centered pathway.

The reactivity of camphorketene (**2**) is apparently unique. Despite being constrained to the reactive *s-Z* conformation[2,4] it does not participate in [4 + 2] trapping reactions observed with other α-oxoketenes.[2,4] However, it dimerizes through a [4 + 2] pathway,[5,6] similarly to other α-oxoketenes.[4] Either the reactivity of **2** toward benzaldehyde is reduced, or the reactivity toward dimerization is increased. Since **2** has been observed in solution at room temperature,[7] we favor the former explanation. We reasoned that strain in the camphor moiety of **2** should pull the ketene and ketone functionalities further apart than in the corresponding *s-Z*-formylketene **8** and thus reduce its reactivity, particularly toward carbonyl compounds and imines.

To explore this possibility, geometry optimizations of **8**[16] and **9** (the latter as a desmethyl model of **2**) were performed at the B3LYP density function level[17] with the 6-31G* basis set using Gaussian 94.[18] The optimized structures are shown in Figure 2. The distance between the reactive centers (C2 and O5) was calculated to be approximately 0.17 Å longer for **9** as compared to **8**. A similarly long distance in camphorketene **2** would make it more difficult for typical dieneophilic traps (e.g.,

(8) X-ray data: monoclinic space group P21, a = 11.549(3), b = 13.860(3), c = 12.352(2) Å, _ = 98.97(2)°, V = 1952.8 Å^3, Z = 4. Independent data: 4652 (R_{int} = 0.0317) wR2 = 0.1019 [$I > 2$ or (I)], the asymmetric unit consisted of two chemically identical molecules but with slightly different conformations (see Supporting Information).

(9) Sterically hindered α-oxoketenes undergo [4 + 2] cycloadditions in which the oxo group participates as the two-atom component. (a) Kappe, C. O.; Evans, R. A.; Kennard, C. H. L.; Wentrup, C. *J. Am. Chem. Soc.* **1991**, *113*, 4234−4237. (b) Kappe, C. O.; Farber, G.; Wentrup, C.; Kollenz, G. *J. Org. Chem.* **1992**, *57*, 7078−7083.

(10) Unpublished results from this lab.

(11) Sato, M.; Ogasawara. H.; Yoshizumi, E.; Kato, T. *Chem. Pharm. Bull.* **1983**, *31*, 1902−1909.

(12) After the completion of this work, a solid-phase method for the preparation of dilute solutions of ketenes was reported that might have simplified our procedure. Hafez, A. M.; Taggi, A. E.; Wack, H., III; W. J. D.; Lectka, T. *Org. Lett.* **2000**, *2*, 3963−3965.

(13) (a) Andraos, J.; Kresge, A. J.; Peterson, M. R.; Csizmadia, I. G. *J. Mol. Struct.* **1991**, *232*, 155−177. (b) Andraos, J.; Chiang, Y.; Kresge, A. J.; Popik, V. V. *J. Am. Chem. Soc.* **1997**, *119*, 8417−8424.

(14) Birney, D. M.; Wagenseller, P. E. *J. Am. Chem. Soc.* **1994**, *116*, 6262−6270.

(15) (a) Allen, A. D.; Andraos, J.; Kresge, A. J.; McAllister, M. A.; Tidwell, T. T. *J. Am. Chem. Soc.* **1992**, *114*, 1878−1879. (b) Chiang, Y.; Guo, H.-X.; Kresge, A. J.; Tee, O. S. *J. Am. Chem. Soc.* **1996**, *118*, 3386-3391. (c) Chiang, Y.; Kresge, A. J.; Meng, Q.; Moriata, Y.; Yamamoto, Y. *J. Am. Chem. Soc.* **1999**, *121*, 8345−8351.

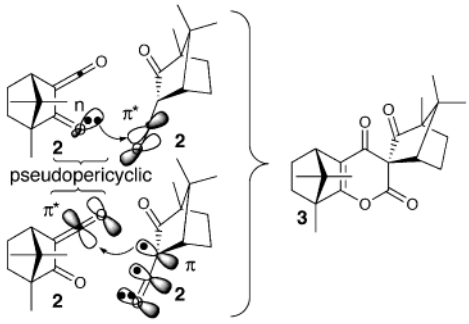

Figure 1. Proposed orbital overlap in the dimerization of **2**. The participating orbitals on the left-most molecule of **2** do not overlap with the extended π-system; thus the reaction is pseudopericyclic.

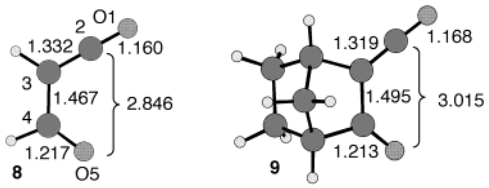

Figure 2. B3LYP/6-31G* optimized geometries of **8** and **9**. Distances shown are angstoms. Carbons are gray, hydrogens are white, and oxygens are speckled.

benzaldehyde) to bond in a [4 + 2] pathway. The dimerization may be favored due to the 0.1 Å longer bond length of the C−C double bond of the ketene (C2−C3) compared to that of the carbonyl moiety (C4−O5).

The NMR spectra of esters **5**,[7] **6**, and of acid **7** all show a mixture of endo and exo products. The endo and exo isomers were not completely separable by HPLC. The sterically less crowded endo isomer is the major one in each case.[19] Interestingly, the NMR spectra, including DEPT-135, showed no evidence for enol formation. This result is consistent with the findings of Wentrup who also reported no enol.[7] Given that β-keto esters often have significant populations of enols, lack of enol formation is at first surprising. However, significant populations of the enol tautomer require hydrogen bonding between the ester carbonyl oxygen and the enol hydroxyl.[20] This suggests that the strain of the camphor moiety also pulls the carbonyl and the enol too far apart for effective hydrogen bonding. Additionally, strain tends to shorten exocyclic bonds,[20,21] (as is evident in comparing **8** with **9** in Figure 2) which would disfavor the enol. Both of these factors could thus contribute to the observed lack of enol tautomers for **5**, **6**, and **7**.

Camphor derivatives often show remarkable facial selectivities, even at fairly remote sites. For example, camphorsultam acrylates show high facial selectivities in Diels−Alder reactions (100% de after recrystallization).[3a] How can it then be that this [4 + 2] dimerization forming a new sterogenic center at the core of the camphor skeleton, proceeds with only 2:1 selectivity? This seems unlikely to be a concerted Diels−Alder reaction with bond formation between the two π faces.

We would suggest that the minimal diastereoselectivity is because the bonding in the transition state does not involve the out-of-plane π-face of the molecule of **2** which is the four-atom component of the [4 + 2] cycloaddition. Rather, this molecule is expected to react in a pseudopericyclic fashion with bonds forming in the plane of the α-oxoketene as shown in Figure 1.[14] We have previously shown that there is essentially no diastereoselectivity in [4 + 2] reactions of chiral α-oxoketenes.[2b] Furthermore, the two-atom component is reacting as a ketene. In analogy to other reactions of ketenes, initial bond formation here again is expected to occur in the plane of the ketene, while only later would the other bond begin to form with the out-of-plane π face.[22]

To provide additional insight into this hypothesis, a transition structure (**10**) was calculated for the dimerization of **8**, as a model for the dimerization of **2**. While this does not reflect the strain of **2** nor steric congestion in the formation of **3**, it should reproduce the essential electronic effects of the transition state. In addition, the product **11** was calculated. These structures are shown in Figure 3. As predicted above, the transition structure **10** involves bond formation in the plane of the molecule of **8** that acts as the four-atom component, as is clearly seen in views A and C. The shorter of the forming bonds (O5−C2′, 2.061 Å) is in the plane of both ketenes. The two forming bonds are almost orthogonal (view B; the O5−C2′−C3′−C2 dihedral is 68°) as expected for the electrophilic and nucleophilic reaction sites on a ketene. Thus the transition structure accommodates both the planar, pseudopericyclic geometry favored by α-oxoketenes and the orthogonal geometry favored by ketenes.

The calculated barrier height (B3LYP/6-31G* + ZPE) is 10.2 kcal/mol, which is comparable to the calculated barriers for the additions of water and formaldehyde (6.3 and 10.6 kcal/mol, respectively, at the MP4(SDQ)/6-31G* + ZPE//MP2/6-31G* level). The overall reaction is calculated to be moderately exothermic (22.8 kcal/mol). This may be compared to the calculated exothermicity of the addition of formaldehyde to **8** (25.3 kcal/mol)[14] and the experimental exothermicity of the parent Diels−Alder reaction (40.8 kcal/mol).[23] The transition structure is somewhat early and asynchronous, with forming bonds

(16) Formylketene has been studied by a number of groups, at a variety of theoretical levels. We recalculated it at the B3LYP/6-31G* level for consistent comparison with the other calculations reported herein. (a) Nguyen, M. T.; Ha, T.; More O'Ferrall, R. A. *J. Org. Chem.* **1990**, *55*, 3251−3256. (b) Birney, D. M. *J. Org. Chem.* **1994**, *59*, 2557−2564. (c) Wong, M. W.; Wentrup, C. *J. Org. Chem.* **1994**, *59*, 5279−5285. (d) Koch, R.; Wong, M. W.; Wentrup, C. *J. Org. Chem.* **1996**, *61*, 6809−6813. (e) Koch, R.; Wong, M. W.; Wentrup, C. *J. Org. Chem.* **1997**, *62*, 1908. (f) Eisenberg, S. W. E.; Kurth, M. J.; Fink, W. H. *J. Org. Chem.* **1995**, *60*, 3736−3742. (g) Anglada, J. M.; Bofill, J. M. *J. Org. Chem.* **1997**, *62*, 2720−2726. (h) Badawi, H. M.; Förner, W.; Al-Saadi, A. *J. Mol. Struct. (THEOCHEM)* **2000**, *505*, 19−30.

(17) Becke, A. D. *J. Chem. Phys.* **1993**, *98*, 5648−5652.

(18) Frisch, M. J.; Trucks, G. W.; Schlegel, H. B.; Gill, P. M. W.; Johnson, B. G.; Robb, M. A.; Cheeseman, J. R.; Keith, T.; Petersson, G. A.; Montgomery, J. A.; Raghavachari, K.; Al-Laham, M. A.; Zakrzewski, V. G.; Ortiz, J. V.; Foresman, J. B.; Peng, C. Y.; Ayala, P. Y.; Chen, W.; Wong, M. W.; Andres, J. L.; Replogle, E. S.; Gomperts, R.; Martin, R. L.; Fox, D. J.; Binkley, J. S.; Defrees, D. J.; Baker, J.; Stewart, J. P.; Head-Gordon, M.; Gonzalez, C.; Pople, J. A. Gaussian 94, Revision B.3; Gaussian, Inc.: Pittsburgh, PA, 1995.

(19) The endo isomer was identified by coupling of the exo hydrogen to the bridgehead (J = 5 Hz) as well as W-coupling (J = 2 Hz).

(20) Carey, F. A.; Sundberg, R. J. *Advanced Organic Chemistry, Part A: Structure and Mechanism*; Plenum Press: New York, 1990.

(21) (a) Wiberg, K. B.; Bader, R. F. W.; Lau, C. D. H. *J. Am. Chem. Soc.* **1897**, *109*, 1001−1012. These effects have been recently utilized to stabilize planar cyclooctatetraenes. (b) Baldrige, K. K.; Siegel, J. S. *J. Am. Chem. Soc.* **2001**, *123*, 1755−1759. (c) Matsuura, A.; Komatsu, K. *J. Am. Chem. Soc.* **2001**, *123*, 1768−1769.

(22) Simple ketenes generally undergo initial bond formation in-plane at the central carbon.[4b]

(23) Tardy, D. C.; Ireton, R.; Gordon, A. S. *J. Am. Chem. Soc.* **1979**, *101*, 1508−1514.

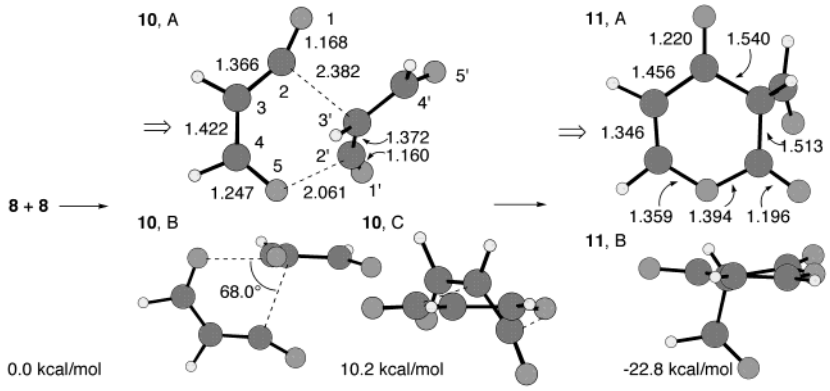

Figure 3. B3LYP/6-31G* optimized geometries of the transition state (**10**) for dimerization of **2** and of the cycloadduct **12**. See Figure 2 for key. Energies are relative to two molecules of **8** and include unscaled ZPE corrections. For **10**, view A is orthogonal to the plane of the four-atom component **8**, view B is looking down the ketene O1′═C2′═C3′ moiety of the two-atom component **8** (O5−C2′−C3′−C2 dihedral shown), and view C is looking from the arrow shown in view A. For **11**, view A is orthogonal to the ring and view B is from the arrow.

of 2.061 and 2.382 Å (O5−C2′ and C2−C3′ respectively). A similar geometry was calculated for the transition structure for the [4 + 2] cycloaddition of **8** and *s-E*-formylketene (as the four- and two-atom components, respectively) and is shown in the Supporting Information.

X-ray Structures. Ground-state geometries of molecules in a reactive conformation can show distortions toward transition states.[24] One of the first and most significant examples of this was the pioneering study of nucleophilic additions to carbonyl compounds by Burgi and Dunitz.[24a] In their study of the anomeric effect, Jones and Kirby examined a series of acetals and found a linear relationship between bond length and reactivity toward solvolysis.[24b] Recently, Pool and White reported similar distortions toward retro-Diels−Alder transition states in Diels−Alder adducts constrained to boat conformations.[24c] The X-ray structure of **3** shows a similar distortion, not toward a conventional Diels−Alder transition state, but toward the calculated planar, pseudopericyclic transition state for the retro-[4 + 2] dimerization of **2**. The complete details of the X-ray structure determination are available in the Supporting Information; selected bond angles and distances are shown in Figure 4A.

Figure 4B shows deviations from average bond angles and distances in model substructures. For these comparisons, substructure searches were performed on the Cambridge Structural Database (CSD).[25] Selected average bond distances and angles are shown in Figure 5. Substructure **12** is an average of 59 relatively unstrained structures that were selected out of 81 structures in the database that matched the substructure; substructure **13** is an average of 18 structures.

Substructure **12** (Figure 5) was designed to see if there is an inherent effect on the bond distances caused by the interaction of an ester and a ketone through a quaternary carbon; these structures were not restricted to lactones.

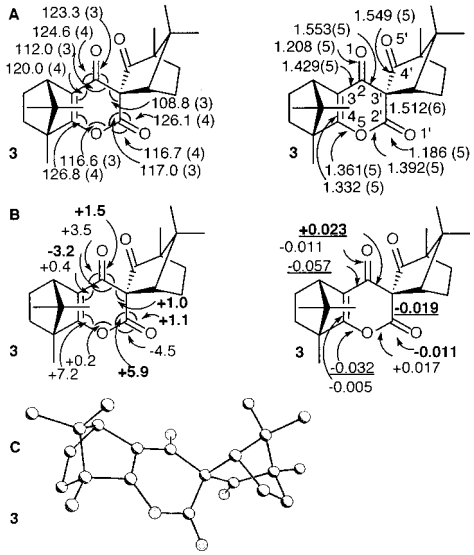

Figure 4. (A) Selected bond angles (degrees) and distances (Å) from the X-ray crystal structure of **3**.[8] Atom numbering follows **8** (Figure 2B). (B) Deviations from average bond distances and angles in **12** (in bold) or **13**, from searches of CSD on these substructures. The underlined bonds are exocyclic to strained rings and thus are expected to be shortened. (C) X-ray structure of **3**.

There does not seem to be a significant effect. The bonds from the quaternary carbon to the two carbonyls are of similar average lengths (1.530 and 1.531 Å). The ester C═O bonds are a bit shorter than the ketone ones (1.195 vs 1.219 Å). The angles to the carbonyl groups are fairly similar 123.0° and 121.7° for the ketone and 123.5° and 125.0° for the esters.

Substructure **13** was chosen to explore the interactions of a ketone with an enol ester, but without the cyclic interaction in **3**. Thus the one other similar ketene dimer[26] (**19**, Figure 7) in the database was excluded from these averages. As might be expected, the ketone in **13** is lengthened by conjugation (1.219 Å) as is the ester

(24) (a)Burgi, H. B.; Dunitz, J. D.; Shefter, E. *J. Am. Chem. Soc.* **1973**, *95*, 5065−5067. (b) Jones, P. G.; Kirby, A. J. *J. Chem. Soc., Chem. Commun*. **1979**, 288−289. (c) Pool, B. R.; White, J. M. *Org. Lett*. **2000**, *2*, 3505−3507. (d) Uehara, F.; Sato, M.; Kaneko, C.; Kurihara, H. *J. Org. Chem*. **1999**, *64*, 1436−1441. (e) Structural manifestations of stereoelectronic and anomeric effects are discussed at length in Deslongchamps, P. *Stereoelectronic Effects in Organic Chemistry*, 1st ed.; Pergamon Press: Oxford, 1983. We have also seen similar distortions in ab initio geometries of ground-state molecules. (f) Birney, D. M.; Ham, S.; Unruh, G. R. *J. Am. Chem. Soc.* **1997**, *119*, 4509−4517. (g) Birney, D. M. *J. Am. Chem. Soc.* **2000**, *122*, 10917−10925.

(25) CSD Version 5.20 (Oct. 2000) Allen, F. H.; Davies, J. E.; Galloy, J. J.; Johnson, O.; Kennard, O.; Macrae, C. F.; Mitchell, E. M.; Mitchell, G. F.; Smith, J. M.; Watson, D. G. *J. Chem. Inf. Comput. Sci*. **1991**, *31*, 187−204.

(26) Kappe, C. O.; Farber, G.; Wentrup, C.; Kappe, T. *Chem. Ber.* **1993**, *126*, 2357−2360.

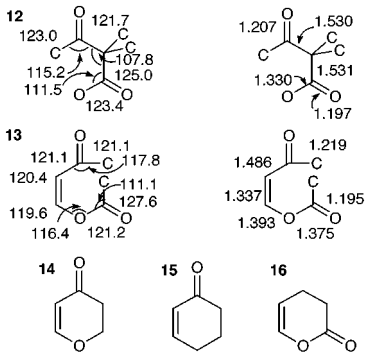

Figure 5. Average bond angles and distances from substructure searches of the Cambridge Structural Database. See text for details and Supporting Information for angles and distances of **14**, **15**, and **16**.

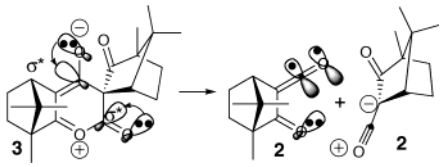

Figure 6. Proposed orbital interactions leading to a planar, pseudopericyclic transition state for the retro-[4 + 2] cycloaddition of **3**.

C−O (1.375 Å) as compared to **12**. The angles to the ester carbonyl are now different, 121.2° and 127.6 Å, with the ester carbonyl tilting toward the divalent oxygen. A similar trend was noted in a series of X-ray structures of mesionic compounds (**17**) for which Wentrup interpreted the geometries as reflecting contributions from ring-opened ketene resonance structures (**18**).[27]

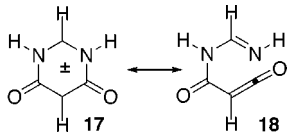

Average geometries of substructures **14**, **15**, and **16** are provided in the Supporting Information for comparison to the more inclusive substructure **13**. The average bond distances and angles in **13** would appear to result from the cumulative effects of the enol ether ketone **14** and the enol lactone **16**.

Figure 4B compares the average geometries in substructures **12** and **13** with the geometry of **3**. In discussing the geometry of **3**, it is important to consider the effects of the ring strain of the camphor moieties on the central ring. In general, ring strain in a molecular system leads to lengthening of the endocyclic bonds and shortening of the exocyclic bonds due to changes in the hybridization of the ring atoms.[20,21] These distortions are also evident in the geometries calculated for the ketenes **8** and **9** (Figure 2) in which the strain in **9** increases the bond alternation in the α-oxoketene moiety. Thus the bonds that are exocyclic to the camphor rings in **3** (underlined in Figure 4B) should be shortened as compared to those of **12** and **13**. All of the distortions in Figure 4B are consistent with a no-bond resonance contribution of two camphorketenes (**2**), as discussed below. It should be noted that dimerization of **2** is only formally reversible; pyrolysis of **3** leads to a rearranged product.[6]

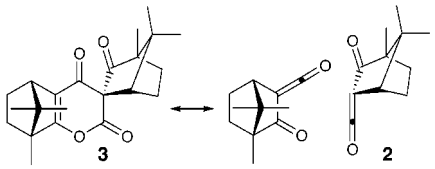

The most remarkable distortion in the X-ray structure of **3** is the lengthening of the C2−C3′ bond. Not only is this bond significantly longer (0.023 Å) than in the unstrained comparison structure **12**, but this lengthening is contrary to the expected shortening from strain since this bond is exocyclic to a camphor moiety. The C2′−O5 bond is also lengthened by 0.017 Å as compared to substructure **13**.

The C2−C3 and C4−C5 bonds in **3** are even more dramatically shortened (0.057 and 0.032 Å, respectively). These bonds are exocyclic to a camphor moiety and so are expected to shorten. One might expect the strain-induced shortening to be similar in the two bonds. However, the C2−C3 bond is shortened by 0.025 Å more than the C4−C5 bond. This difference must be attributed to something other than strain; again it is consistent with a contribution from a ketene in the no-bond resonance structure.

The C2′−C3′ distance in **3** is shortened by 0.019 Å as compared to **12**. This distance would be expected to be shortened by strain and by distortion toward the ketene. It is not possible to dissect the contributions from the two effects in this case, but it is not inconsistent with the latter.

The C3−C4 bond distance in **3** should be lengthened both by strain in the camphor and by the single bond contribution in the ketene. It is formally 0.005 Å shorter in **3** than in **13**. However, this is within experimental error, the same as in the comparison substructures **12** and **13**. We have no explanation for this, other than to suggest that this bond is the farthest from the breaking bonds and thus might not be expected to show any significant distortions. However, we also note that this bond length is apparently relatively insensitive to environment, varying by no more than 0.007 Å between **13**, **14**, **15**, and **16**.

The two carbonyl groups in **3** (O1−C2 and O1′−C2′) are both shortened by 0.011 Å as compared to the model substructures **12** and **13**. This is consistent with a distortion toward the ketene structures. It would also then be expected that the carbonyl groups should be tilted. Tilting is evident in the O1′−C2′ carbonyl group of **3**. The O1′−C2′−O5 angle is reduced by 4.5° as compared to a substructure **13** while the O1′−C2′−C3′ angle is opened by 1.1° as compared to **12**. It should be noted that the O1′−C2′−C3′ angle in **3** is smaller than the comparable angle in **13**; this is not as expected for a distortion toward the ketenes. At the O1−C2 carbonyl of **3**, tilting would increase the steric crowding between O1 and the camphor moiety. Thus, it is understandable that the O1−C2−C3′ angle in **3** is slightly increased (1.5°) as compared to **12**. Nevertheless, the larger increase in the O1−C2−C3 angle of 3.5° as compared to **13** is

(27) Plüg, C.; Wallfisch, B.; Andersen, H. G.; Bernhardt, P. V.; Baker, L.-J.; Clark, G. R.; Wong, M. W.; Wentrup, C. *J. Chem. Soc., Perkin Trans. 2* **2000**, 2096−2108.

consistent with the proposed distortion toward ketenes. Also, this latter angle in **3** is larger than in **12**.

Comparisons of interior angles is complicated by the geometrical constraints of the rings and thus will not be discussed in detail. Strain in **3** would be expected to open the C2−C3−C4, C3−C4−O5 and C2−C3′−C2′ angles, as is found; these are opened by 0.4°, 7.2°, and 1.0°, respectively. That the C3−C2−C3′ angle is reduced by 3.2° and the C3′−C2′−O5 angle is opened by 5.9° may both be consequences of the other distortions in the molecule.

Compound **11** (the dimer of **8**) lacks the angle strain of **3**, but it should still have the same electronic factors as **3**. Indeed, the calculated structure of **11** (Figure 3) shows similar ground-state distortions. The C2−C3′ and C2′−O5 bonds are long while the C2′−C3′ and C4−O5 bonds are short. The C2−C3 bond is calculated to be longer in **11** than is observed in **3**, as expected due to strain in **3**. Overall though, the structure of **11** suggests that the strain in **3** has at most small effects on the bond lengths. The detailed agreement between the calculated and observed structures gives additional confidence in the calculations.

These ground-state distortions of **3** and of **11** may also be viewed as manifestations of a type of stereoelectronic effect[24c,d,e] in which lone pairs from the carbonyl oxygens can donate electron density into the σ^* orbitals of the breaking bonds, as illustrated in Figure 6. A possible contributor to this effect would be the charge-separated resonance structure shown, in which the α-oxoketene π-system is already in place. Fragmentation then simply forms the in-plane lone pair and π-bond of **2** shown. These may be recognized as essentially the same orbital interactions proposed for the pseudopericyclic formation of **3** in Figure 1.

Indeed, the most important aspect of the geometry of **3** and of **11** is that the central pyrandione ring is almost completely planar. For **3**, the mean displacement from the plane is only 0.13 Å. However, if the ground state of **3** is distorted toward a fragmentation, as judged by the changes in bond distances and angles, then together these two observations strongly suggest that the transition state for dimerization of **2** is planar. This result is in dramatic contrast to the nonplanar (π-face to π-face) transition states predicted for hydrocarbon [4 + 2] cycloadditions[28] and the trends observed in their ground-state geometries.[24c] Planar transition states are predicted for sigmatropic rearrangements of allylic esters,[29] for electrocyclic ring openings of furylcarbenes,[30] for cycloadditions of α-oxoketenes,[14] and for the dimerization of **2**; the distortions in the X-ray structure of **3** provides the most direct experimental verification of these theoretical predictions to date!

The experimental structure of **3** and the calculated structure of **11** are both distorted; we interpret these distortions as being toward the transition state. The obvious question is "why should these, or any other structures,[24a−c] distort along an endothermic reaction path?" From other work,[24a,b,d,e,g] it is clear that there is a direct, and sometimes linear,[24b] relationship between the heat of reaction and the distortions, in accord with the Hammond Postulate.[31] Nevertheless, these distortions are real, even in endothermic reactions.[24a−d] We suggest that the same orbital interactions that give rise to the low barriers for dimerization of **2** (10.2 kcal/mol) and **8** remain in **3** and **11** and are thus manifest in the structural distortions.

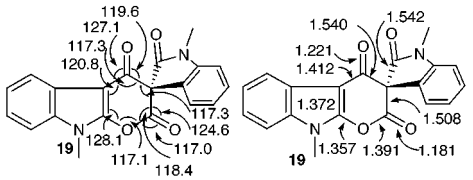

Figure 7. Selected bond distances and angles from the X-ray structure of **19**.

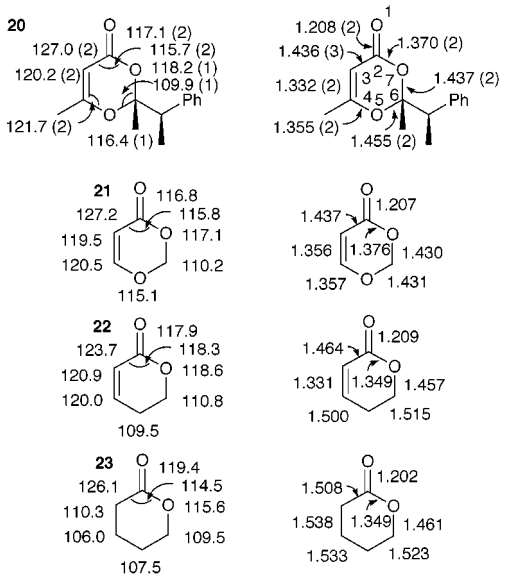

Figure 8. Selected bond angles and distances of **20** and averages from substructure searches of the CSD.

Similar trends in bond distances and angles are seen in the X-ray structure of **19**, the only other related dimer of an α-oxoketene in the CSD, shown in Figure 7.[26] We note that the C2−C3′ and C2′−O5 bonds are long (1.540 and 1.391 Å, respectively) and the C2−C3 and C4−O5 bonds are short (1.412 and 1.357 Å, respectively) as expected for the no-bond resonance contribution. The C3−C4 bond in **19** is longer than in **3**, but it is part of an aromatic ring and thus is not directly comparable. Lacking the steric crowding of **3**, the O1−C2−C3 angle in **19** is larger (127.1°) and the O1−C2−C3′ angle is smaller (119.6°) as expected for tilting the carbonyl toward the ketene. Again, the central ring is close to planar, indicating that the ground-state distortions toward the no-bond structure are consistent with a planar pseudopericyclic transition state.

Finally, we have examined the structures of a series of dioxinones, (Figure 8) including compound **20** for which we previously determined the X-ray structure.[2b] Substructure **21** is based on averages of 6 other dioxinones[32] from the CSD, **22** an average of 56 compounds and **23** an average of 301 compounds. Dioxinones can be formed by the cycloaddition of an α-oxoketene with a carbonyl compound and these structures also show distortions toward planar, pseudopericyclic transition states. Specif-

(28) Woodward, R. B.; Hoffmann, R. *The Conservation of Orbital Symmetry*; Verlag Chemie, GmbH: Weinheim, 1970.

(29) Birney, D. M.; Xu, X.; Ham, S. *Angew. Chem., Int. Ed.* **1999**, *38*, 189−193.

(30) Birney, D. M. *J. Am. Chem. Soc.* **2000**, *122*, 10917−10925.

(31) Hammond, G. S. J. *J. Am. Chem. Soc.* **1955**, *77*, 334−338.

ically, the C2−O7 distances are longer than in comparable lactones (1.370 Å in **20** and 1.376 Å in **21** as compared to 1.349 Å in both **22** and **23**). Similarly, in **20** the O5−C6 bond is longer (1.455 Å) than the C6−O7 bond (1.437 Å), while these bonds are essentially of equal length in **21**. The carbonyl is also tipped, reflecting a contribution from the ketene structure; the O1−C2−C3 bond angle is 127.0° in **20** and 127.2° in **21**, while it is only 123.7° in **22**. the O1−C2−O7 angle is 117.1° in **20** and only 116.8° in **21**, while it is 117.9° in **22**. Since **20** and **21** are close to planar, these geometric distortions are all indicative of distortions toward planar, pseudopericyclic transition states in these systems as well.

In conclusion, the stereochemistries of the camphorketene (**2**) dimers **3** and **4**, first synthesized in 1920 by Staudinger, have finally been determined. The X-ray crystal structure of **3**, **19**, **20**, and **21** are all distorted toward planar, pseudopericyclic transition states for retro [4 + 2] cycloadditions, in agreement with theoretical calculations. These structures provide the most direct experimental evidence to date regarding this unusual transition state geometry. The distortions are also interpreted in terms of stereoelectronic effects involving the same orbital interactions as the pseudopericyclic pathway. The surprising lack of diastereoselectivity in the dimerization of **2** is also consistent with the pseudopericyclic pathway. The calculated transition structure **10** reflects both planar, pseudopericyclic orbital overlap on the 4-atom α-oxoketene and orthogonal bonding on the 2-atom ketene fragment. Trapping of **2** with alcohols shows chemoselectivity comparable to other α-oxoketenes. However, **2** does not display typical α-oxoketene reactivity toward benzaldehyde, or benzaldimine, despite being constrained to the reactive *s-Z* conformation. This and the lack of enol tautomers of **5**, **6**, or **7** are attributed to a longer C2−O5 distance resulting from strain in **2**. Over 80 years after it was first synthesized, the study of camphorketene (**2**) continues to provide new insights into α-oxoketene chemistry and also into pseudopericyclic reactions in general.

Experimental Section

NMR spectra were recorded in $CDCl_3$ (^1H at 300 or 500 MHz, and ^{13}C at 50 or 75.47 MHz) using $CHCl_3$ as an internal standard. ^1H and ^{13}C NMR spectra were consistent with the proposed structures. COSY and DEPT spectra were obtained for **3**, **5**, and **6** to confirm the assignments. Chemical shifts are reported in ppm, couplings in Hz. Toluene and ether were distilled from Na prior to use. Other reagents were used as received. Products were purified by flash chromatography on silica gel (hexane/ethyl acetate eluents) unless otherwise noted.

D-(+)-3-Camphoric Acid (**7**).[5] In a 250 mL three-neck flask toluene (25 mL) and D-(+)-camphor (2.0 g, 1.3 mmol) were cooled to −78 °C. LDA (16.0 mL, 2.6 mmol, 2 M) was added and stirred at −78 °C for 15 min. The resultant solution was then allowed to warm to room temperature and then poured into an excess of dry ice and stirred until all dry ice disappeared. The reaction was then worked up by adding water (35 mL) and extracting with ether. The basic aqueous layer was acidified with dilute HCl and reextracted with ether. The organic layer was dried over $MgSO_4$ and the excess solvent evaporated. Yield = 96% mixture of endo and exo.

Endo diastereomer. ^1H NMR (300 MHz in $CDCl_3$) δ 0.86 (s, 3H), 0.93 (s, 3H), 1.00 (s, 3H), 1.48 (m, 1H), 1.56 (m, 1H), 1.71 (m, 1H), 1.89 (m,1H), 2.46 (t, 1H, J = 4.5 Hz), 3.35 (dd, J = 8 Hz, 3.5 Hz, 1H), 9.07 (s,1H). ^{13}C NMR (125 MHz in $CDCl_3$) δ 9.34, 18.61, 19.57, 22.34, 29.96, 45.63, 46.58, 55.52, 58.49, 173.17, 213.39.

D-(+)-3-Camphoryl Chloride (**1**).[5] In a 100 mL round-bottom flask D-(+)-3-camphoric acid (**7**, 2.3 g 1.17 mmol) was placed and the flask cooled to −4 °C in an ice bath. Thionyl chloride (10 mL) was added. The reaction was stirred at −4 °C for 12 h. Excess thionyl chloride was evaporated with a vacuum pump. The resultant yellow oil was washed with petroleum ether. The petroleum ether was subsequently removed by rotary evaporation. Yield = 95% mixture of endo and exo.

α-Oxocamphorketene Dimers (**3** and **4**).[5] In a 100 mL round-bottom flask diethyl ether (20 mL) and triethylamine (2.5 mL, 1.8 mmol) were placed. Camphoryl chloride (**1**, 2.0 g, 0.93 mmol) was added and the resultant reaction stirred for 30 min. The reaction was worked up in diethyl ether and washed successively with sodium bicarbonate and brine solutions. The organic layer was dried over $MgSO_4$ and the excess solvent evaporated. The crude product was repeatedly recrystallized from diethyl ether. Yield = 20%.

Dimer 3 (minor): Optical rotation α_D + 135° (in $CHCl_3$) (α_D + 126° in EtOAc);[5] ^1H NMR (500 MHz in $CDCl_3$) δ 0.91 (s, 3H), 1.03 (s, 3H), 1.06 (s, 9H), 1.17 (s, 3H) 1.23 (m, 2H), 1.60 (m, 1H), 1.80 (m, 3H), 1.78 (m, 1H), 2.13 (m, 1H), 2.71 (d, 1H, J = 6 Hz), 2.83 (d, 1H, J = 6.0 Hz). ^{13}C NMR (125 MHz in $CDCl_3$) δ 8.74, 9.68, 18.61, 19.45, 21.01, 21.90, 25.86, 26.64, 29.77, 32.92, 47.52, 48.17, 54.13, 54.49, 55.13, 58.59, 74.70, 120.04, 168.79, 173.14, 185.81, 206.89.

Dimer 4 (major): Recrystallized from MeOH. Decomposed on standing.[6] ^1H NMR (300 MHz in $CDCl_3$) δ 0.85 (s, 3 H), 0.94 (s, 3H), 0.95 (s, 3H), 0.97 (s, 3H), 0.99 (s, 3H), 1.04 (s, 3H), 1.48 (m, 2H), 1.72 (m, 3H), 1.81 (m, 1H), 2.00 (m, 1H), 2.28 (t, j = 3.9 Hz, 1 H), 2.47 (d, J = 3.6 Hz, 1H), 3.26 (dd, 1H).

Attempted Reaction of D-(+)-3-Camphoryl Chloride (1) and Benzaldehyde. In a 100 mL round-bottom flask diethyl ether (25 mL), benzaldehyde (0.24 mL, 0.18 mmol), and triethylamine (0.50 mL, 3.4 mmol) were placed. Camphoryl chloride (**1**, 0.38 mL, 0.18 mmol) was added. The resultant solution was stirred for 30 min. The reaction was worked up with diethyl ether and washed successively with sodium bicarbonate and brine solutions. No adduct with benzaldehyde was obtained.

Attempted Reaction of D-(+)-3-Camphoryl Chloride (1) and *N*-Propylbenzaldimine. In a 100 mL round-bottom flask diethyl ether (25 mL), *N*-propylbenzaldimine (147 mg, 0.10 mmol), and triethylamine (0.25 mL, 1.9 mmol) were placed. Camphoryl chloride (**1**, 0.21 mL, 0.10 mmol) was added. The resultant solution was stirred for 30 min. The reaction was worked up with diethyl ether and washed successively with sodium bicarbonate and brine solutions. No adduct with propylbenzaldimine was obtained.

D-(+)-Isopropyl 3-Camphorcarboxylate (**6**). In a 100 mL round-bottom flask camphoryl acid chloride (**1**, 0.14 g, 0.07 mmol) and diethyl ether (20 mL) were placed. To this solution 2-propanol (0.10 mL, 0.13 mmol) and triethylamine (0.46 mL, 3.3 mmol) were added simultaneously. The resultant reaction was stirred for 20 min and then quenched with water. The reaction was worked up with diethyl ether and washed successively with sodium bicarbonate and brine solutions. The organic layer was dried over $MgSO_4$ and the excess solvent evaporated.

D-(+)-Isopropyl 3-Camphorcarboxylate (6) and D-(+)-Methyl 3-Camphorcarboxylate (5).[7] See Table 1 for product ratios and yields.

Method 1. In a 100 mL round-bottom flask camphoric acid chloride (**1**, 0.14 g, 0.07 mmol), and diethyl ether (20 mL) were placed. To this solution 2-propanol (0.36 mL, 0.47 mmol),

(32) (a) Vilsmaier, E.; Joerg, K.; Maas, G. *Chem. Ber.* **1984**, *117*, 2947−2962. (b) L'Abbe, G.; Bastin, L.; Dehaen, W.; Toppel, S.; Delbeke, P.; Vilaghe, D.; Meervelt, D. V. *J. Chem. Soc., Perkin Trans. 1* **1994**, 2545−2551. (c) Richie, K. A.; Bowsher, D. K.; Popinski, J.; Gray, G. M. *Polyhedron* **1994**, *13*, 227−233. (d) Sato, M.; Murakami, M.; Sunami, S.; Kaneko, C.; Furuya, T.; Kurihara, H. *J. Am. Chem. Soc.* **1995**, *117*, 4279−4287. (e) Sato, M.; Uehara, F.; Kamaya, H.; Murakami, M.; Kaneko, C.; Furyua, T.; Kunihara, H. *J. Chem. Soc., Chem. Commun.* **1996**, 1063−1066.

methanol (0.76 mL, 1.9 mmol), and triethylamine (0.46 mL, 3.3 mmol) were added simultaneously. The resultant reaction was stirred for 20 min and then quenched with water. The reaction was worked up with diethyl ether and washed successively with sodium bicarbonate and brine solutions. The organic layer was dried over $MgSO_4$ and the excess solvent evaporated.

Method 2. In a 100 mL round-bottom flask camphoric acid chloride (**1**, 0.10 g, 0.05 mmol), and diethyl ether (20 mL) were placed. To this solution 2-propanol (0.025 mL, 0.36 mmol) and methanol (0.045 mL, 1.1 mmol) was added. The resultant reaction was stirred for 20 min and then quenched with water. The reaction was worked up with diethyl ether and washed successively with sodium bicarbonate and brine solutions. The organic layer was dried over $MgSO_4$ and the excess solvent evaporated.

Method 3. Using a modification of method 1,2-propanol/methanol mixture in the molar ratio of 1:3.23 was used as the solvent in place of diethyl ether. Yield = 96% based on crude NMR.

D-(+)-Isopropyl 3-Camphorcarboxylate (6). Endo diastereomer. ^{1}H NMR (500 MHz in $CDCl_3$) δ 0.87 (s, 3H), 0.95 (s, 3H), 1.02 (s, 3H), 1.25 (d, 3H, J = 6 Hz) 1.26 (d, 3H, J = 6 Hz), 1.55 (m, 2H), 1.69 (m, 1H), 1.71 (m, 1H), 2.43 (t, 1H, J = 4.5 Hz), 3.30 (dd, J = 5 Hz, 2 Hz, 1H), 5.07 (sept, 1H, J = 6 Hz). ^{13}C NMR (125 MHz in $CDCl_3$) δ 9.52, 18.81, 19.48, 21.77, 21.80, 22.35, 29.36, 45.70, 47.05, 55.73, 55.49, 68.42, 169.20, 211.57. Exo diastereomer. ^{1}H NMR (500 MHz in $CDCl_3$) δ 0.80 (s, 3H), 0.96 (s, 3H), 0.98 (s, 3H), 1.26 (d, 3H, J = 6 Hz) 1.28 (d, 3H, J = 6 Hz), 1.40 (m, 1H), 1.55 (m, 1H), 1.71 (m, 1H), 2.03 (m, 1H), 2.63 (t, 1H, J = 4.5 Hz), 2.84 (s, 1H), 5.03 (sept, 1H, J = 6 Hz). ^{13}C NMR (125 MHz in $CDCl_3$) δ 9.46, 19.44, 20.81, 21.62, 21.65, 27.38, 30.11, 45.99, 46.75, 57.58, 58.74, 68.74, 167.25, 211.1

D-(+)-Methyl 3-Camphorcarboxylate (5).[7] Endo diastereomer. ^{1}H NMR (500 MHz in $CDCl_3$) δ 0.85(s, 3H), 0.91 (s, 3H), 0.99 (s, 3H), 1.51 (m, 2H), 1.67 (m, 1H), 1.84 (m, 1H), 2.40 (t, 1H, J = 4.5 Hz), 3.31 (dd, J = 5 Hz, 2 Hz, 1H), 3.69 (s,3H). ^{13}C NMR (125 MHz in $CDCl_3$) δ 9.42, 18.69, 19.41, 22.39, 29.30, 45.60, 46.95, 55.43, 58.49, 68.42, 169.20, 211.57. Exo diastereomer. ^{1}H NMR (500 MHz in $CDCl_3$) δ 0.75(s, 3H), 0.92 (s, 3H), 0.95 (s, 3H), 1.37 (m, 1H), 1.51 (m, 1H), 1.67 (m, 1H), 2.02 (m, 1H), 2.62 (d, 1H, J = 4.5 Hz), 2.85 (s, 1H), 3.71 (s,3H). ^{13}C NMR (125 MHz in $CDCl_3$) δ 9.37, 19.30, 20.63, 27.21, 30.01, 45.89, 46.67, 57.70, 57.48, 68.5, 168.20, 210.8.

Computational Methods. All calculations were performed at the B3LYP/6-31G*[17] level using the Gaussian 94 suite of programs.[18] Geometries were fully optimized with no constraints. The nature of the stationary points was verified by frequency calculations; all transition structures had only one imaginary frequency that corresponded to the proposed reaction coordinate. Absolute energies are reported in the Supporting Information. Relative energies include unscaled zero-point vibrational energy corrections. In addition to **10** and **11**, a transition structure was located for the [4 + 2] cycloaddition of **8** and *s-E*-formylketene. The *s-E*-conformation is not accessible in camphorketene. This reaction is calculated to have a barrier of 9.5 kcal/mol and an exothermicity of 21.4 kcal/mol. Structures and energies are provided in the Supporting Information.

Acknowledgment. We thank the Robert A. Welch foundation for support of this work, the NSF (grant no. CHE-9808436) for partial funding of the 500 MHz NMR spectrometer, the High Performance Computing Center at Texas Tech University for computer time, and Professor Jonathan M. White for helpful discussions.

Supporting Information Available: Figures, B3LYP/6-31G* optimized Cartesian coordinates and a table of absolute energies for **8**, **9**, **10**, and **11** as well as for the cycloaddition of **8** and *s-E*-formylketene. X-ray data for **3**. ^{1}H and ^{13}C NMR spectra of **3**, **4**, **5**, **6**, and **7**. This material is available free of charge via the Internet at http://pubs.acs.org.

JO015698T